Low mass dileptons as fireball thermometer at HADES energies

F. Seck[2], T. Galatyuk[1,2], R. Rapp[3] and J. Stroth[4,2]

[1]TU Darmstadt, Darmstadt, Germany; [2]GSI, Darmstadt, Germany; [3]Texas A&M University, College Station (TX), USA; [4]Goethe Universität, Frankfurt, Germany;

The systematic study of dilepton production in heavy-ion collisions across a large range of collision energies makes it possible to link experimental observables like yields and slopes of the spectra to features (phase transition(s) and possible critical point) in the QCD phase diagram. As dileptons are emitted during the whole space-time evolution of the collision, the resulting spectra comprise several contributions from first-chance NN collisions, the hadronic freeze-out cocktail, but also thermal radiation which serves as messenger of the QCD matter properties inside the hot and dense medium.

We couple in-medium thermal dilepton rates with a coarse-graining method of hadronic transport simulations to compute dilepton spectra at SIS18 beam energies, where hydrodynamic simulations may be less reliable. After checking the degree of thermalization of the system, local temperature, baryon and pion densities can be extracted in the nearly equilibrated parts of the fireball. This allows for the convolution of thermal rates with the space-time evolution of the medium.

The slope of the invariant-mass spectrum of thermal dilepton radiation in the intermediate mass region (IMR) between the ϕ and the J/Ψ mesons can be utilized as a thermometer of the fireball. If the electromagnetic spectral function $\mathrm{Im}\Pi_{\mathrm{em}}/\mathrm{M}^2$ is constant, the shape of the spectrum is given by $\frac{\mathrm{dN}}{\mathrm{dM}} \sim (\mathrm{MT})^{3/2} \exp(-\mathrm{M}/\mathrm{T})$. To good approximation, this is true for the IMR [1, 2]. The observed temperature necessarily represents an average over the space-time evolution of the fireball. It is however dominated by the radiation emanating from the hottest stage reached during the collision.

Since the invariant-mass is Lorentz-invariant, the extracted temperature is not affected by a blue shift caused by the radial expansion of the medium.

In heavy-ion collisions at beam energies in the SIS18 range the conditions reached during the evolution comprise high baryon densities of several times normal nuclear matter density and temperatures up to 85 MeV.

Under those environments there are strong medium modifications to the spectral function of the ρ meson [3]. This leads to an almost structureless spectrum [4] as shown in figure 1.

At energies accessible to the HADES experiment at SIS18, the IMR is hard to access. The statistics collected during the Au+Au beamtime with 1.23A GeV collision energy in the year 2012 was not enough to populate the spectrum above the ϕ meson with sufficient yield. Theoretical modelling predicts T ~ 85 MeV, corresponding to the hottest space-time cells in the evolution [4, 5].

Due to the strong medium effects, $\mathrm{Im}\Pi_{\mathrm{em}}/\mathrm{M}^2$ is also reasonably flat in the mass range 0.3-0.7 GeV/c^2 as shown in figure 2.

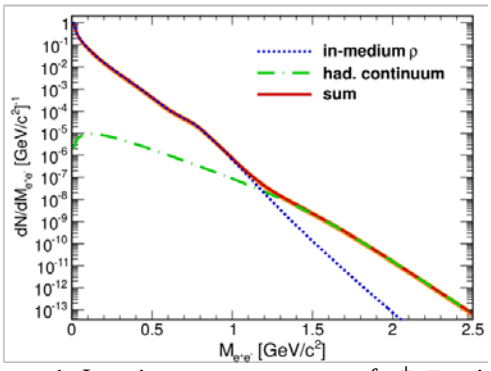

Figure 1: Invariant-mass spectrum of e^+e^- pairs radiated from a central Au+Au collision at 1.23A GeV [4].

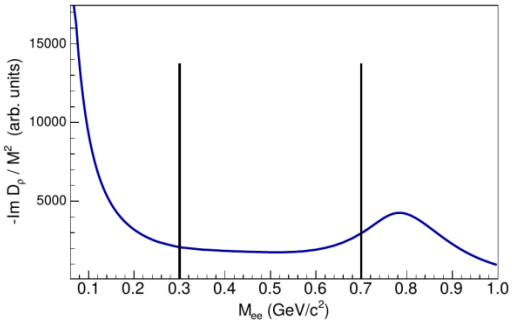

Figure 2: In-medium ρ spectral function $\mathrm{Im}\ \mathrm{D}_\rho/\mathrm{M}^2$ averaged over different temperatures and baryon densities as they occur during the space-time evolution.

This allows the use of the low mass region (LMR) for the temperature measurement instead.

As the suppression from the thermal Boltzmann factor is weaker at lower masses, the radiation in this mass region is not restricted to the hottest stage and more cells with different conditions can contribute. This leads to an extracted temperature which is ~ 20MeV lower, indicating that the measurement integrates over a longer time interval in the space-time evolution of the medium.

The upcoming Ag+Ag beamtime of HADES at a slightly higher collision energy will make it possible to test this relation between the temperatures extracted from the IMR and the LMR in experiment.

References

[1] R. Rapp and H. van Hees, PLB 753 (2016) 586
[2] H. Specht (NA60), AIP Conf. Proc. 1322 (2010) 1
[3] R. Rapp and J. Wambach, EPJ A 6 (1999) 415
[4] T. Galatyuk et. al, EPJ A 52 (2016) 131
[5] F. Seck et. al, arXiv: 1710.06256

Grants: VH-NG-823, DFG through grant CRC-TR 211
Strategic university co-operation with: Darmstadt

The dark matter axion mass

G. D. Moore[1], *V. B. Klaer*

[1]IKP, TU Darmstadt, Germany

Introduction

A major potential link between particle physics and cosmology is the nature of dark matter. One of the most interesting dark matter candidates is the axion, a pseudo-Goldstone boson whose existence would explain the observed time-reversal symmetry of QCD.

Highly coherent, nearly-at-rest axions can be created in the early Universe, and they make an ideal dark matter candidate. If we can establish how efficient this process is, we can relate the axion mass to the axion's role as dark matter. If we assume that:

1) the axion exists;
2) PQ symmetry is restored in the early Universe or the axion field otherwise starts out randomly different through space;
3) the axion makes up all of the dark matter,

then we are able to make a unique prediction for the axion mass.

Methodology

The axion Lagrangian in terms of a complex scalar field

$$\mathcal{L} = g^{\mu\nu}\partial_\mu\varphi\partial_\nu\varphi + \frac{m^2}{8f_a^2}\left(2\varphi^*\varphi - f_a^2\right)^2 + \chi(T)(1-\cos\theta_a) \quad (1)$$

can be solved directly as a real-time classical field theory, with random initial conditions for the scalar field, via lattice methods. The dynamics is rich because the scalar field can contain topological structures called axionic strings; close to such a string, in cylindrical coordinates, the field obeys

$$\varphi = f(r)f_a e^{i\theta_a}, \quad \theta_a = \pm\phi \quad (2)$$

such that the scalar changes by plus or minus 2pi in winding one time around in azimuth. The energy associated with such a string diverges at short distances as the logarithm of distance, cut off by the inverse of the mass in the Lagrangian. This distance is of order 30 orders of magnitude shorter than the inter-string separation, giving rise to a logarithmically large string tension for such strings. But numerical simulations cannot reproduce this, because both scales must be resolved on the lattice which cannot be much larger than 2000 points across. Therefore simulations feature strings with approximately 10 times too small a tension.

We resolve this problem, and thereby present reliable simulations of axion production in the early Universe, by proposing a model with additional massive degrees of freedom, which are only active in the string core and which give rise to a much higher value for the string tension, with otherwise the same long-distance axionic dynamics. We do this by studying a theory with two complex scalars with different charges, and a single U(1) gauge field; one linear combination of fields is the axion, the other couples to the gauge field and forms abelian-Higgs strings. Each string has both an axionic and an abelian-Higgs character, with the abelian Higgs component contributing only to its tension, which we can therefore tune. Details of the method are presented in [1] and the cosmological results are presented in [2].

The most significant result is that the axion production is *smaller* than it would be, under the approximation that each region of space has a different starting angle and evolves independently (the misalignment approximation). The axion number increases as one increases the string tension, but quite weakly, as shown in Figure 1.

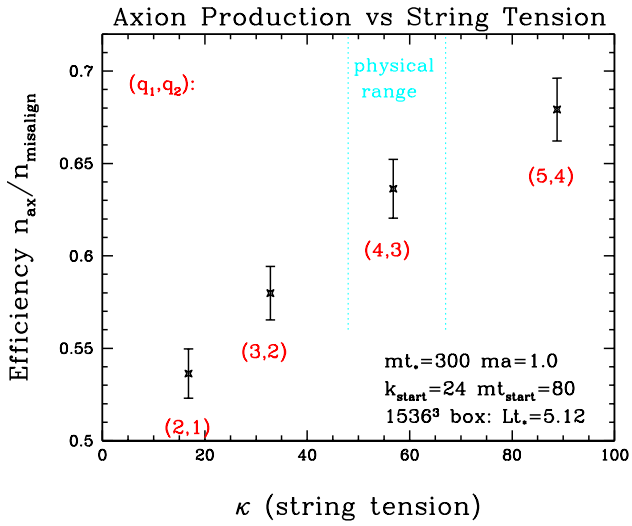

Figure 1: Axion production efficiency (relative to the misalignment approximation) as a function of the extra contribution to the string tension (the log of the scale separation we want to simulate).

Based on these results, we are able to establish the axion decay constant, and axion mass, for which the axions would make up 100% of the dark matter. Specifically, with the assumptions mentioned in the introduction, we find that the axion mass should be 26.2 plus or minus 3.4 micro-electron volts. This prediction narrows the frequency range experiments must explore.

References

[1] V. B. Klaer and G. D. Moore, "How to simulate global cosmic strings with large string tension," JCAP 1710, Oct. 2017, article 043.

[2] V. B. Klaer and G. D. Moore, "The dark-matter axion mass," JCAP 1711, Oct. 2017, article 049.

Strategic university co-operation with Darmstadt

 DOI:10.15120/GR-2018-1

Transport coefficients of quark matter from the Kubo formalism

A. Harutyunyan[1], D. H. Rischke[1], and A. Sedrakian[2]

[1]ITP, D-60438 Frankfurt-Main, Germany, [2]FIAS, D-60438 Frankfurt-Main, Germany

The transport coefficients of quark plasma are important input parameters for the hydrodynamical simulations of heavy-ion collision experiments. In this context, we have computed all first order transport coefficients of two-flavor quark plasma close to the critical temperature of chiral phase transition. The quark matter is described within the two-flavor Nambu Jona-Lasinio model which is well-suited for studies of chiral phase transitions [1, 2].

The transport coefficients are extracted from the Kubo type formulas by evaluating the specific correlation functions required for the electrical and thermal conductivities as well as shear and bulk viscosities. We apply the $1/N_c$ expansion in order to truncate the infinite series of Feynman diagrams contributing to the correlation functions and find that the conductivities and the shear viscosity can be described by a single-loop skeleton diagram with full quark propagator. In contrary, the bulk viscosity requires a resummation of a full series of multi-loop diagrams. Close to the critical temperature of chiral phase transition the dispersive effects that lead to nonzero transport coefficients arise from quark-meson fluctuations above the Mott-temperature T_M for meson dissociation.

We find that the conductivities and the shear viscosity are decreasing functions of temperature and density for $T>T_M$, see Fig. 1. These coefficients show a universal behavior as functions of the scaled temperature T/T_M.

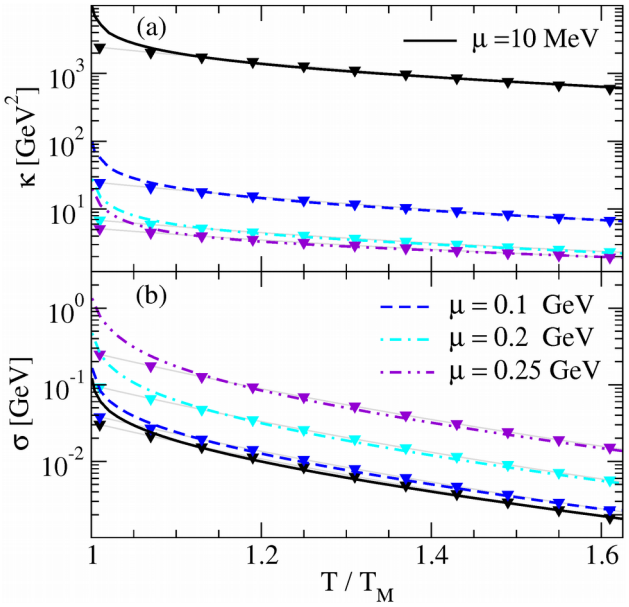

Figure 1: The thermal conductivity κ (a) and the electrical conductivity σ (b) as functions of the scaled temperature T/T_M at several values of the chemical potential. The triangles reproduce the results of the fit formulas.

The case of the bulk viscosity turns out to be special, because the multi-loop contributions ζ_1 and ζ_2 dominate the single-loop contribution ζ_0 close to the Mott line in the case where the chiral symmetry is explicitly broken, see Fig. 2. We find that in this case only at high temperatures the one-loop contribution becomes dominant. The resulting bulk viscosity has a mild minimum as a function of temperature and exceeds the shear viscosity close to the Mott temperature by factors 5 ÷ 20 when multi-loop contributions are included. In the high-temperature domain

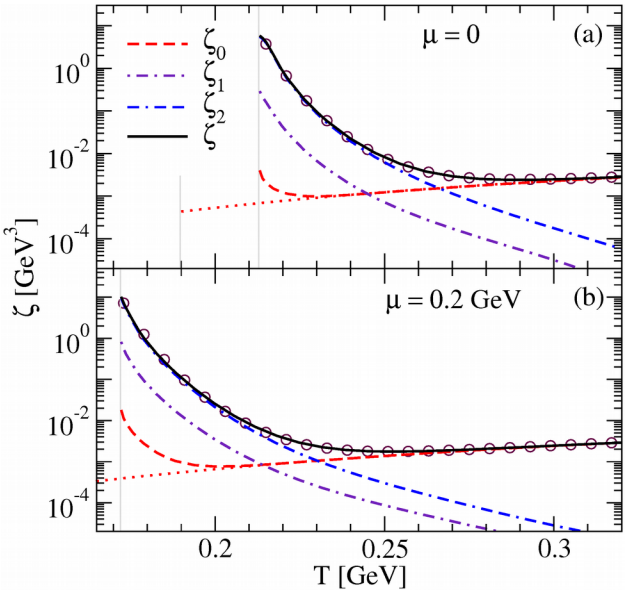

the bulk viscosity is negligible compared to the shear viscosity.

For practical applications we provide simple fits to the transport coefficients, which can facilitate the implementation of our results in hydrodynamic simulations.

Figure 2: Three components of the bulk viscosity and their sum as functions of temperature for two values of the chemical potential. The dotted lines correspond to the chiral limit. The results of the fits are shown by circles.

References

[1] A. Harutyunyan, D. H. Rischke and A. Sedrakian, Transport coefficients of two-flavor quark matter from the Kubo formalism, Phys. Rev. D 95 (2017) 114021, [1702.04291].

[2] A. Harutyunyan and A. Sedrakian, Bulk viscosity of two-flavor quark matter from the Kubo formalism, Phys. Rev. D 96 (2017) 034006, [1705.09825].

Strategic university co-operation with: Frankfurt-M

Influence of the axial anomaly on the decay $N(1535) \to N\eta$

L. Olbrich[1], M. Zétényi[1,2,3], F. Giacosa[1,4], and D. H. Rischke[1,5]

[1]Goethe University, Frankfurt am Main, Germany; [2]Wigner Research Center for Physics, Budapest, Hungary; [3]GSI, Darmstadt, Germany; [4]Jan Kochanowski University, Kielce, Poland; [5]University of Science and Technology of China, Hefei, Anhui, China.

The decay width of $N(1535) \to N\eta$ is as large as that of $N(1535) \to N\pi$. This is surprising, because considering flavor symmetry we would expect that

$$\frac{\Gamma_{\mathrm{N}(1535)\to N\eta}}{\Gamma_{\mathrm{N}(1535)\to N\pi}} \simeq \frac{\cos^2\theta_P}{3} \simeq 0.17\,, \qquad (1)$$

where the factor 3 takes the pion triplet into account and $\theta_P \simeq -44.6°$ [1] is the strange−non-strange mixing angle of the isoscalar-pseudoscalars. [Phase space reduces the ratio in Eq. (1) even further.]

We propose that the axial $U(1)_A$ anomaly is responsible for the enhanced coupling of $N(1535)$ to the η meson. To test this idea, we consider the so-called extended linear sigma model (eLSM). It includes (pseudo)scalar and axial(-vector) mesons [1] as well as glueballs [2] and features the explicit, spontaneous, and anomalous breaking of chiral symmetry. In Refs. [3,4], chirally symmetric Lagrangians describing baryons and their chiral partners in the mirror assignment were constructed for the cases $N_f = 2$ and $N_f = 3$, respectively. Both models cannot reproduce the decay width of $N(1535) \to N\eta$ [as expected because flavor symmetry holds in any chirally symmetric model, and thus Eq. (1) follows].
However, treating baryons in the mirror assignment allows to construct a further term in the baryonic sector, which preserves the chiral $SU(N_f)_L \times SU(N_f)_R$ symmetry but explicitly breaks the axial $U(1)_A$ symmetry, see Ref. [5]. Such anomalous terms induce additional interactions of some baryons and their chiral partners with the η meson.

The eLSM parametrizes (pseudo)scalar mesons via the field $\Phi(x)$, which behaves under chiral transformations as $\Phi \to U_L \Phi\, U_R^\dagger$, where $U_{L(R)} \in U(N_f)_{L(R)}$. Thus, terms involving $\det\Phi$ can be embodied to model the axial anomaly. We consider the following negative-parity term:

$$\det\Phi - \det\Phi^\dagger\ . \qquad (2)$$

Coupling this term to a baryonic field combination (equal to the one of the chirally invariant mass term, which exists only in the mirror assignment), yields a parity-even chiral invariant, see Ref. [5].

For the case $N_f = 2$ [and in the absence of (axial-)vector degrees of freedom], we obtain

$$\det\Phi - \det\Phi^\dagger = -i\,(\sigma_N + \phi_N)\eta_N + i\,a_0\cdot\pi\ , \qquad (3)$$

where we shifted the isoscalar-scalar field σ_N by its non-zero vacuum expectation value ($\sigma_N \to \sigma_N + \phi_N$), which arises from the spontaneous breaking of chiral symmetry. From Eq. (3) it is visible that the coupling of Eq. (2) to a baryonic combination induces a direct coupling of the η meson to some baryons. Indeed, incorporating such an anomalous term into the two-flavor eLSM of Ref. [3], an enhanced decay $N(1535) \to N\eta$ can be obtained by adjusting the respective coupling constant, see Ref. [5].

For the case $N_f = 3$, we consider the eLSM as investigated in Ref. [4], where four baryonic multiplets are present. One can introduce analogous anomalous terms, which enhance the decay of chiral partners into baryons and an η meson. Then, upon identifying $N(1535)$ as the chiral partner of the nucleon and $\Lambda(1670)$ as chiral partner of $\Lambda(1116)$, after fixing the decay width of $N(1535) \to N\eta$, the decay $\Lambda(1670) \to N\eta$ can be correctly described, see Ref. [5]. This approach predicts also a strong $N(1535)N\eta'$ coupling, which is important for studies of η' production processes.

Finally, the developed formalism can be used to couple a pseudoscalar glueball to baryons. We have found that it couples strongly to $N(1535)N$ and possibly to $N(1440)N$, see Ref. [5]. Thus, we expect that the pseudoscalar glueball can be seen in the future PANDA experiment by investigating the process $p + \bar{p} \to p + \bar{p}(1535) + \text{h.c.}$.

References

[1] D. Parganlija, P. Kovacs, G. Wolf, F. Giacosa and D. H. Rischke, Phys. Rev. D 87, 014011 (2013).
[2] W. I. Eshraim, S. Janowski, A. Peters, K. Neuschwander and F. Giacosa, Acta Phys. Polon. Supp. 5, 1101 (2012).
[3] S. Gallas, F. Giacosa and D. H. Rischke, Phys. Rev. D 82 (2010) 014004.
[4] L. Olbrich, M. Zétényi, F. Giacosa and D. H. Rischke, Phys. Rev. D 93 no. 3, 034021 (2016).
[5] L. Olbrich, M. Zétényi, F. Giacosa and D. H. Rischke, Phys. Rev. D 97 (2018) no.1, 014007.

Experiment beamline: none
Experiment collaboration: none
Experiment proposal: none
Accelerator infrastructure: none
PSP codes: none
Grants: HGS-HIRe/HQM, Hungarian OTKA Fund No. K109462, HIC for FAIR, OPUS project no. 2015/17/B/ST2/01625, High-End Visiting Expert project GDW20167100136 (SAFEA), DFG grant no. RI1181/6-1
Strategic university co-operation with: Frankfurt-M, Kielce, Budapest

 DOI:10.15120/GR-2018-1

Clustering in pre-compound nuclei in the TDDFT framework

B. Schuetrumpf [1,2] W.Nazarewicz [3]

[1]GSI, Darmstadt, Germany; [2]Institut für Kerphysik, Technische Universität Darmstadt; [3]FRIB Laboratory, Michigan State University

Clustering in atomic nuclei is a ubiquitous phenomenon. Although it is commonly accepted to be very important for many aspects, it is hard to describe and detect in numerical simulations. Earlier works showed, that clustering can be revealed in nuclear mean-field calculations by the nucleonic localization function (NLF), which was adapted from quantum chemistry. In this work the NLF is applied to time-dependent density functional theory (TDDFT) calculations of collisions of intermediate mass nuclei. A special focus is put on the early stage of the collision, where -in contrast to the equilibrated compound nucleus- the freshly fused system (or pre-compound nucleus) still carries a strong imprint of the entrance channel of the collision.

Usually TDDFT calculations are analyzed using predominantly the nucleon density distribution. Examples of snapshots of the time evolution are shown in Fig. 1 left panels. However, the density contains only little information of the internal structure of the nucleus. On the other hand, the NLF, which is based on the inverse probability of finding two nucleons with same spin and isospin in the vicinity of each other (Fig. 1 right panels), reveal distinct regions with localizations close to 1, signaling the presence of clusters. Regions of high localizations at the tips as in Fig. 1 (b) mark alpha clusters, since for an alpha particle the probability of finding two nucleons with same spin and isospin close to each other vanishes. Other clusters like carbon clusters containing 6 neutrons and 6 protons manifest in ring structures. That can be easily verified by analyzing the nucleon content of the cluster regions. In our study it was found that the collision of two oxygen nuclei at a center of mass energy of around 20 MeV results in a pre-compound system where two alpha particles oscillate against two carbon clusters

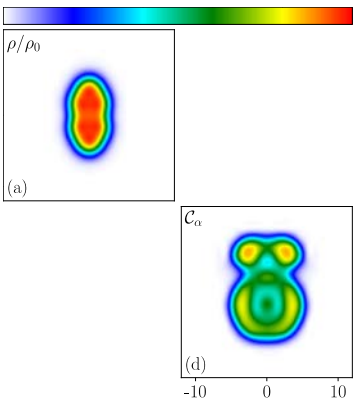

[1].Figure 1: Snapshots of oxygen + oxygen (top) and calcium + oxygen (bottom) TDDFT simulations of central collisions. Total densities normalized to nuclear saturation density ((a) and (c)) and nucleon localization ((b) and (d)). Collisions is cylindrically symmetric w.r.t. the z=0 axis. Taken from [1].

Not only central collisions, but also collisions with a non-zero impact parameter were carried out. The alpha-C-C-alpha structure displayed in Fig. 1 (b) is shown in Fig. 2 for different impact parameters. While for the central collision the system conserves axial symmetry, for b > 0 the alpha clusters shift slightly into the direction of rotation thus creating more overlap with the carbon clusters, resulting in a lower localization. However, the overall structure of the state remains up to high impact parameters.

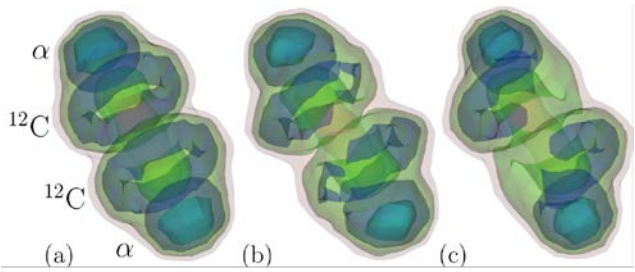

Figure 2: Alpha-C-C-alpha structure in oxygen + oxygen for the central collision (a), with b=2 fm (b), and b=4 fm (c). Taken from [1].

A study of oxygen + carbon collisions around the Coulomb barrier reveals extreme alpha clustering for all impact parameters where (intermediate) fusion occurs [1]. This supports experimental studies [2], which have detected enhanced alpha emission in those reactions. The authors of [2] find that statistical models underestimate the alpha emission strongly for those reactions. The results suggest, that the cluster structure of the initial fragment nuclei gives rise to strong entrance channel effects, neglected by the statistical models. This influences the alpha emissions following fusion.

In summary it has been shown that the NLF provides a useful measure to reveal clustering also in the time-dependent formalism. The assumption of a fully equilibrated compound nucleus in such reactions is incomplete and entrance channel effects play an important role, especially in reactions with short contact time. With the help of the NLF clusters can be traced and, with significant modifications and beyond mean-field techniques the emission probabilities could be extracted in future works.

References

[1] B. Schuetrumpf and W. Nazarewicz, Phys. Rev. C **96**, 064608 (2017)

[2] J. Vadas, T. K. Steinbach, J. Schmidt, V. Singh, C. Haycraft, S. Hudan, R. T. deSouza, L. T. Baby, S. A. Kuvin, and I. Wiedenhöver, Phys. Rev. C **92**, 064610 (2015).

Strategic university co-operation with: TU Darmstadt

Dilepton production in carbon-carbon collision in comparison to HADES measurements

J. Staudenmaier[1,2] and H. Petersen[1,2,3]

[1]GSI, Darmstadt, Germany; [2]Johann Wolfgang Goethe-Universität, Frankfurt am Main, Germany; [3]Frankfurt Instiute for Advanced Studies (FIAS), Frankfurt am Main, Germany

Electromagnetic probes offer the unique possibility to gain undisturbed insights into strongly interacting matter produced by nucleus-nucleus collisions. This includes lepton pairs (dileptons) that are, for the here discussed low energy reactions, predominantly produced by decays of resonances. Therefore, they offer the possibility to study resonance properties within a hadronic medium. In-medium changes to these properties e.g. the spectral function have been discussed to reveal features of the theory of the strong interaction (QCD) such as chiral symmetry restoration [1].

However, before probing in-medium properties, a solid baseline description for di-lepton production in absence of a medium needs to be established. This is possible in the context of the rich experimental data set from HADES with elementary reactions and small nucleus-nucleus reaction, which represent a superposition of elementary reactions.

The approach chosen for this work is a new hadronic transport model: SMASH (=Simulating Many Accelerated Strongly-interacting Hadrons) [2]. As a transport model, it is based on the relativistic Boltzmann equation. The collision term is emulated by decays and binary collisions using a geometric collision criterion. All well-known resonance from the PDG [3] up to a mass of 2.3 GeV are included. Di-leptons are produced by decays of various resonance. This work focuses on di-electron production, for which mesonic decays of $\pi, \eta, \rho, \omega, \phi$ and baryonic decays from the Δ resonance are included. New in this approach are contributions to the direct vector meson decay channels below the hadronic thresholds, which equals the combined mass of the lightest hadronic decay products [4].

Results for the di-electron production in carbon-carbon collisions at E_{Kin} = *2.0A* GeV are shown in Figure 1. In the invariant mass spectrum the dominant contribution for masses below 500 MeV are the pseudo-scalar meson π and η decays. Above 500 MeV the vector meson channels are dominant. ρ and ω contributions below the hadronic threshold, which for the ρ is at two π masses, are observed. The ρ contribution is the second largest contribution around 250 MeV. The agreement with experimental data [5] is excellent. Only around the ω pole a slight overestimation is seen.

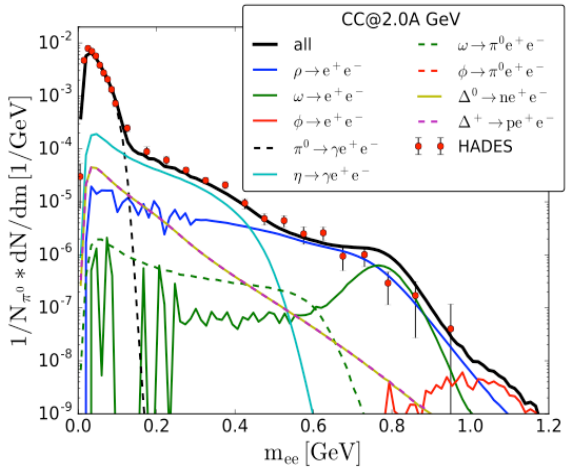

Figure 1: Invariant mass spectrum of di-electrons produced by carbon-carbon collisions at E_{Kin} = *2.0A* GeV compared to HADES data from [5].

On this solid description of smaller systems, the dilation production for larger systems can be studied. The vector meson contributions are sensitive to modification to the spectral function, since they decay directly into a lepton pair. With HADES data available also for larger system it is possible to probe for which systems the assumption of vacuum properties remains valid and for which the invariant mass spectrum of di-leptons is senstive to medium modifications.

References

[1] R. Rapp, J. Wambach, and H. van Hees, Landolt-Bornstein 23, 134 (2010), arXiv:0901.3289 [hep-ph].

[2] J. Weil et al, Phys.Rev. C94 (2016) no.5, 054905

 DOI:10.15120/GR-2018-1

[3] K. A. Olive et al. (Particle Data Group), Chin. Phys. C38, 090001 (2014).
[4] J. Staudenmaier et al, J.Phys.Conf.Ser. 832 (2017) no.1, 012037
[5] G. Agakishiev et al. (HADES), Eur. Phys. J. A40, 45 (2009), arXiv:0902.4377 [nucl-ex].

Experiment beamline: HADES
Experiment collaboration: CBM / HADES
Experiment proposal: [e.g. S339] none
Accelerator infrastructure: SIS18 / SIS100 / CERN-LHC
PSP codes: [none]
Grants: Work supported by Helmholtz Nachwuchsgruppe VH-NG-822, by the LOEWE Initiative HIC for FAIR of the State of Hesse and GSI. Computational resources have been provided by the Center for Scientific Computing (CSC) at the Goethe-University of Frankfurt and the GreenCube at GSI. J.S. acknowledges support by the Deutsche Forschungsgemeinschaft (DFG) through the grant CRC-TR 211 “Strong-interaction matter under extreme conditions”.
Strategic university co-operation with: Frankfurt-M / FIAS

Lattice QCD investigation of the structure of the $a_0(980)$ meson

J. Berlin[1], M. Wagner[1] in collaboration with *C. Alexandrou[2,3], M. Dalla Brida[4], J. Finkenrath[3], T. Leontiou[5]*

[1]Goethe-Universität Frankfurt am Main, Institut für Theoretische Physik, Max-von-Laue-Straße 1, D-60438 Frankfurt am Main, Germany
[2]Department of Physics, University of Cyprus, P.O. Box 20537, 1678 Nicosia, Cyprus
[3]Computation-based Science and Technology Research Center, The Cyprus Institute, 20 Kavafi Street, 2121 Nicosia, Cyprus
[4]Dipartimento di Fisica, Universita di Milano-Bicocca and INFN, Sezione di Milano-Bicocca, Piazza della Scienza 3, I-20126 Milano, Italy
[5]Department of Mechanical Engineering, Frederick University, 1036 Nicosia, Cyprus

We have investigated the quark content of the low-lying states in the $I(J^P) = 1(0^+)$ sector, which are the quantum numbers of the $a_0(980)$ meson, using lattice QCD (for details cf. our recent publication [1]).

We have considered correlation functions of six different two- and four-quark interpolating fields:

$$\mathcal{O}^1 = \mathcal{O}^{q\bar{q}} = N_1 \sum_{\mathbf{x}} \left(\bar{d}(\mathbf{x})u(\mathbf{x})\right)$$

$$\mathcal{O}^2 = \mathcal{O}^{K\bar{K},\ \text{point}} = N_2 \sum_{\mathbf{x}} \left(\bar{s}(\mathbf{x})\gamma_5 u(\mathbf{x})\right)\left(\bar{d}(\mathbf{x})\gamma_5 s(\mathbf{x})\right)$$

$$\mathcal{O}^3 = \mathcal{O}^{\eta_s\pi,\ \text{point}} = N_3 \sum_{\mathbf{x}} \left(\bar{s}(\mathbf{x})\gamma_5 s(\mathbf{x})\right)\left(\bar{d}(\mathbf{x})\gamma_5 u(\mathbf{x})\right)$$

$$\mathcal{O}^4 = \mathcal{O}^{Q\bar{Q}} = N_4 \sum_{\mathbf{x}} \epsilon_{abc}\left(\bar{s}_b(\mathbf{x})(C\gamma_5)\bar{d}_c^T(\mathbf{x})\right) \epsilon_{ade}\left(u_d^T(\mathbf{x})(C\gamma_5)s_e(\mathbf{x})\right)$$

$$\mathcal{O}^5 = \mathcal{O}^{K\bar{K},\ \text{2part}} = N_5 \sum_{\mathbf{x},\mathbf{y}} \left(\bar{s}(\mathbf{x})\gamma_5 u(\mathbf{x})\right)\left(\bar{d}(\mathbf{y})\gamma_5 s(\mathbf{y})\right)$$

$$\mathcal{O}^6 = \mathcal{O}^{\eta_s\pi,\ \text{2part}} = N_6 \sum_{\mathbf{x},\mathbf{y}} \left(\bar{s}(\mathbf{x})\gamma_5 s(\mathbf{x})\right)\left(\bar{d}(\mathbf{y})\gamma_5 u(\mathbf{y})\right)$$

We have evaluated all diagrams, including diagrams, where quarks propagate within a timeslice, e.g. with closed quark loops. A necessary preparatory step was the comparison of the efficiency of various methods to compute two-point correlation functions of two-quark and four-quark interpolating fields of different structure, including combinations of point-to-all propagators, stochastic timeslice-to-all propagators, the one-end trick and sequential propagators (cf. Ref. [2]).

We have demonstrated that diagrams containing such closed quark loops have a drastic effect on the final results and, thus, may not be neglected. Our analysis, which has been carried out at unphysically heavy u and d quark mass corresponding to m_{pion} = 296(3) MeV and in a single spatial volume of extent 2.9 fm, shows that in addition to the expected spectrum of two-meson scattering states there is an additional energy level around the two-particle thresholds of K + K and eta + pion. This state in the energy region of 1100 MeV to 1200 MeV is a candidate for the $a_0(980)$ meson. It is predominantly generated by the quark-antiquark interpolating field O^1, but also receives sizable contributions from the diquark-antidiquark interpolating field O^4, i.e. a likely interpretation is that it is mainly a quark-antiquark state with a minor tetraquark component. To some extent this is supported by a previous computation, where we have neglected quark propagation within a timeslice [3]. Then the quark-antiquark interpolating field decouples from the four-quark interpolating fields and an analysis of the four-quark correlation matrix only yields the expected two-meson scattering states.

Our analysis has been performed using AMIAS, a novel statistical method based on the sampling of all possible spectral decompositions of the considered correlation functions, as well as solving standard generalized eigenvalue problems.

References

[1] C. Alexandrou, J. Berlin, M. Dalla Brida, J. Finkenrath, T. Leontiou and M. Wagner, "Lattice QCD investigation of the structure of the $a_0(980)$ meson," Phys. Rev. D **97**, 034506 (2018) [arXiv:1711.09815 [hep-lat]].

[2] A. Abdel-Rehim, C. Alexandrou, J. Berlin, M. Dalla Brida, J. Finkenrath and M. Wagner, "Investigating efficient methods for computing four-quark correlation functions," Comput. Phys. Commun. **220**, 97 (2017) [arXiv:1701.07228 [hep-lat]].

[3] C. Alexandrou, J. O. Daldrop, M. Dalla Brida, M. Gravina, L. Scorzato, C. Urbach and M. Wagner, "Lattice investigation of the scalar mesons $a_0(980)$ and kappa using four-quark operators," JHEP **1304**, 137 (2013) [arXiv:1212.1418 [hep-lat]].

 DOI:10.15120/GR-2018-1

Nucleosynthesis in neutrino-driven supernova ejecta: Influence of variations in the astrophysical conditions and of (α,n) reaction rates

J. Bliss[1], A. Arcones[1,2], F. Montes[3,4], J. Pereira[3,4], M. Witt[1]

[1]TU Darmstadt, Darmstadt, Germany;[2]GSI, Darmstadt, Germany;[3]NSCL, Michigan State University, MI 48824, USA;[4]Joint Institute for Nuclear Astrophysics, Michigan State University, MI 48824, USA

Core-collapse supernovae synthesize lighter heavy elements between Fe up to possibly Ag depending on the properties of the ejected matter. Despite the fast progress in supernova simulations and experimental astrophysics, the astrophysical and nuclear physics uncertainties are still large and can critically influence the nucleosynthesis. Therefore, we address both sources of uncertainty and study their impact on the nucleosynthesis in neutron-rich neutrino-driven supernova ejecta.

To explore the variations in the astrophysical conditions we rely on a steady-state model [1] because a systematic study based only on trajectories from hydrodynamic simulations is computationally expensive. Steady-state models allow to investigate all possible conditions found in current and future supernova simulations. We vary the mass and radius of the proto-neutron star as well as the total luminosity and energy of the neutrinos, which are input parameters in the wind equations, to cover a wide range of astrophysical conditions and calculate the nucleosynthesis [2]. In the final abundances, we identify four abundance patterns (NSE1, NSE2, CPR1, CPR2) by different neutron, alpha, and seed abundances at T = 3 GK. The different nucleosynthesis groups distinguish in the evolution of the nucleosynthesis path and each groups exhibits characteristic abundance patterns and peaks. The abundance patterns of the groups NSE1 and NSE2 are mainly determined during the nuclear statistical equilibrium (NSE) phase and thus rather depend on binding energies and partition functions. The group CPR1 describes the transition between NSE1 or NSE2 to CPR2. After the breakdown of NSE, charged-particle reactions still redistribute the abundances but the nucleosynthesis path cannot overcomes the neutron shell closure at N = 50. Thus, the final abundances are given by Q-values of (α,n) reactions. Within the groups NSE1, NSE2, and CPR1 the nucleosynthesis evolution is similar. In contrary, we find a lot of variations in the final abundances of the nucleosynthesis group CPR2 (see Fig.1) and especially the heaviest synthesized elements vary. Individual charged particle reactions can critically affect the abundance evolution and nuclei heavier than Z~40 are produced.

For neutron-rich conditions, matter mainly evolves towards heavy nuclei by charged-particles reactions, especially (α,n) reactions [3]. None of the relevant (α,n) reactions has been measured in the energy range that is significant for astrophysical conditions in neutrino-driven supernova ejecta. Therefore, the reaction rates included in our nucleosynthesis studies are calculated with theoretical reaction codes based on the statistical Hauser-Feshbach model. The reaction rates contain some uncertainty due to intrinsic technical aspects in the reaction codes and nuclear physics input [4]. To estimate the uncertainty in the (α,n) rates we calculate them using different alpha optical potentials which are the main contribution to the uncertainty for the relevant astrophysical conditions [5]. Moreover, we compare the theoretical reaction rates with the few available measurements of stable nuclei in the absence of relevant experiments. We conclude that the reliability of the theoretical (α,n) rates is not better than a factor of 10.

We investigate the influence of the rate uncertainties on the nucleosynthesis for different astrophysical conditions by varying all (α,n) reaction rates for nuclei between Fe and Rh by factors of 5, 10, and 50 up and down. When the (α,n) rates are reduced (increased) less (more) matter moves towards nuclei beyond Z=38 compared to the case where no rates are varied. This result is robust for different astrophysical conditions unless the nucleosynthesis evolution is close to the valley of stability. We conclude that (α,n) rate uncertainties are crucial for the nucleosynthesis in neutrino-driven supernova ejecta. Thus, more studies are required to identify the individual important reactions whose measurements will contribute to further reduce the nuclear physics uncertainties.

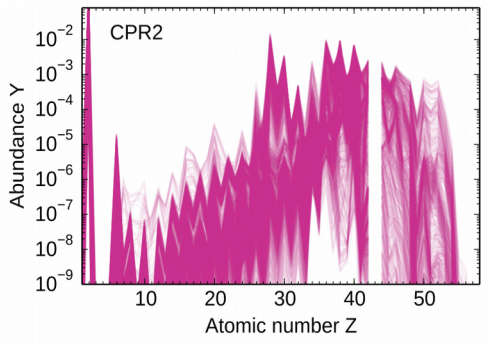

Figure 1: Final abundances of the group CPR2.

Grants: Helmholtz Young Investigator Grant No. VH-NG-825

References

[1] K. Otsuki et al., ApJ 533 (2000) 424.

[2] J. Bliss et al., accepted by ApJ (2018).

[3] S.E. Woosley & R.D. Hoffman, ApJ 395 (1992) 202.

[4] J. Pereira & F. Montes, Phys. Rev. C 93 (2016) 034611.

[5] J. Bliss et al., J. Phys. G: Nucl. Phys. 44 (2017) 054003

Impact of spatial correlations among the proton constituents at LHC energies

J.L. Albacete[1], H.Petersen[2,3,4] and A.Soto-Ontoso[1,2]

[1]Universidad de Granada, Granada, Spain.; [2] FIAS, Frankfurt am Main, Germany, [3] GSI, Darmstadt, Germany, [4] Goethe University, Frankfurt am Main, Germany.

Introduction

The first discovery at the Large Hadron Collider (LHC) occurred in 2010 when two-particle correlations at small relative azimuth angle extending over several units of rapidity were measured in high multiplicity proton-proton (p+p) collisions. This phenomenon, dubbed the ridge, had been previously measured in heavy-ion (A+A) collisions and considered to be a golden probe of quark-gluon plasma (QGP) formation. In addition to the ridge, other QGP-sensitive observables such as the flow harmonic coefficients and their correlations in terms of symmetric cumulants have shown a similar behavior in p+p and in the A+A case [1]. At this point, a natural question arises: are small droplets of QGP being formed in p+p collisions at the TeV regime?

An indispensable ingredient in any theoretical model attempting to describe the striking experimental results is the parametrization of the geometry of the collision.

The model

We propose a description of the proton geometry based on three main ingredients. First, the fundamental constituents of the proton are considered to be gluonic hot spots, by default we consider 3, that can be interpreted in a radiative picture as a valence quark surrounded by a gluonic cloud. Next, the positions of these hot spots in the transverse plane are subjected to short-range repulsive correlations that effectively enlarge the mean transverse separation between them (see Eq.2 in [2]). The inclusion of this effect is the main novelty of this work with respect to others in the literature. Finally, the radius of the hot spot grows with increasing energy of the collision. The theoretical justification for the last two assumptions is given in [3].

We implement this geometry in a Monte Carlo event generator à la Glauber including fluctuations in the hot spots positions and their entropy deposition. The entropy deposition is considered a proxy of particle production and, therefore, is constrained by the experimental data on the charged particle multiplicity distributions. Further, it is the quantity that defines the centrality classes.

Symmetric cumulants

In Fig.1 the correlation between the eccentricity and the triangularity, NSC(2,3) (see Eq.2 in [4]), of p+p collisions at 13 TeV is shown. The most remarkable feature is that the negative sign of NSC(2,3) in the highest centrality bins is only achieved in the correlated scenario [4]. This is the first result in the literature that is, at least, in qualitative agreement with the experimental measurement where the correlation is measured in terms of elliptic and triangular flow.

Together with their drastic impact on the description of the hollowness effect [3] and the absolute values of the eccentricities [2], the symmetric cumulant study adds evidence to the fact that the inclusion of spatial correlations between the sub nucleonic degrees of freedom of the proton modifies the initial state properties of proton-proton interactions at LHC energies.

Figure 1: Normalized symmetric cumulant as a function of the centrality. The light purple band contains the uncorrelated results while the red line corresponds to the correlated scenario.

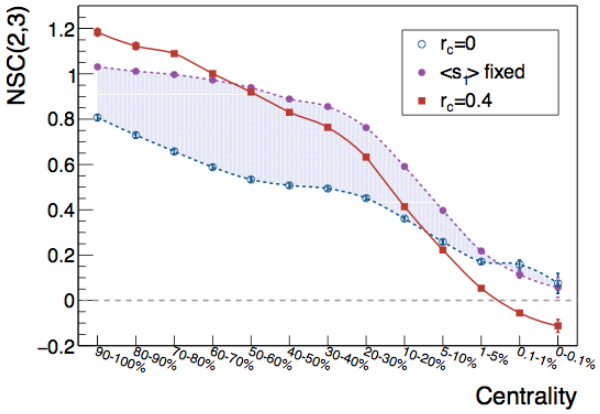

References

[1] CMS Collaboration, “Evidence for collectivity in pp collisions at the LHC”, Phys. Lett. B765 (2017) 193–220 .

[2] J.L.Albacete, H.Petersen and A.Soto-Ontoso, “Correlated wounded hot spots in proton-proton interactions”, Phys.Rev. C95 (2017) no.6, 064909.

[3] J.L.Albacete and A.Soto-Ontoso, “Hot spots and the hollowness of proton-proton interactions”, Phys.Rev. C95 (2017) no.6, 064909.

[4] J.L.Albacete, H.Petersen and A.Soto-Ontoso,“Symmetric cumulants as a probe of the proton substructure at LHC energies”, Phys.Lett. B778 (2018) 128-136.

Grants: Helmholtz Young Investigator Group VH-NG-822, FP7-PEOPLE-2013-CIG Grant of the European Commission QCDense/631558, RYC-2011-09010 and FPA2013-47836.

 DOI:10.15120/GR-2018-1

Baryon number fluctuations in chiral effective models and their phenomenological implications

G. A. Almasi[1], B. Friman[1], and K. Redlich[2,3]

[1]GSI, Darmstadt, Germany; [2]ExtreMe Matter Institute (EMMI), D-64291 Darmstadt, Germany;
[3]University of Wroclaw - Faculty of Physics and Astronomy, PL-50-204 Wroclaw, Poland.

In this work we study the influence of the chiral phase transition on fluctuation observables in strongly interacting matter at non-zero temperature and net baryon density [1]. We focus on the properties of net-baryon-number fluctuations, which are quantified by the baryon number cumulants. These are directly influenced by the chiral phase transition, owing to the coupling of the quarks to the scalar order parameter. Furthermore, since the cumulants can be related to the fluctuations of the net proton number, which are accessible experimentally, they are ideal observables for identifying the phase boundary and critical structures in the QCD phase diagram.

We model chiral dynamics with the Polyakov-loop extended Quark-Meson (PQM) model. To correctly account for the critical behaviour at the chiral symmetry restoration transition in the O(4) and Z(2) universality classes, we employ the Functional Renormalization Group (FRG) [2]. We formulate the FRG equations in the presence of repulsive interactions and derived the flow equations for derivatives of the thermodynamic pressure.

The main focus of our studies is the analysis of the STAR data on proton number fluctuations and the comparison with model predictions. To reduce the influence of the non-critical characteristics of the model, like e.g. the mass spectrum or the kinematical cuts on particle momentum distributions, we compute ratios of susceptibilities. We fix the freeze-out line in our model using the skewness data measured by STAR. By doing so, we qualitatively reproduce the behaviour of all cumulant ratios with multiple parameter sets, except for the rise of the kurtosis at low energies (Fig. 1). We conclude that, since our model calculations do not reproduce this behaviour, this rise cannot be solely attributed to chiral criticality in equilibrium.

We also computed the baryon number cumulants of fifth and sixth order along the freeze-out line. Figure 2 shows that the sixth to second and fifth to first cumulant ratios agree at high beam energies. Since non-equilibrium effects are expected to spoil this relation, we propose to use the ratios of cumulants as probes of equilibration.

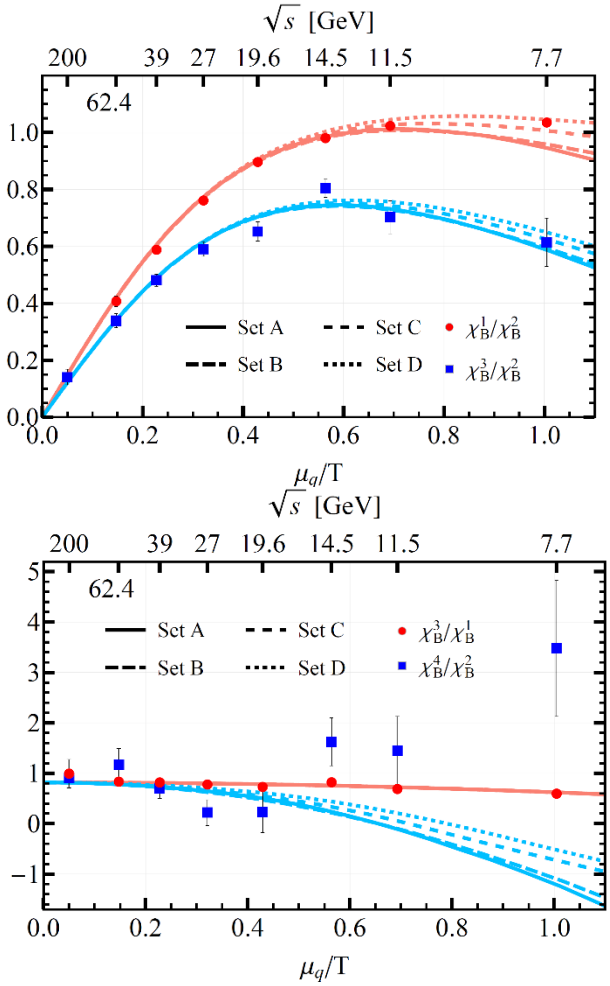

Figure 1: Baryon number cumulant ratios in the PQM model on the freeze-out line fitted to STAR data.

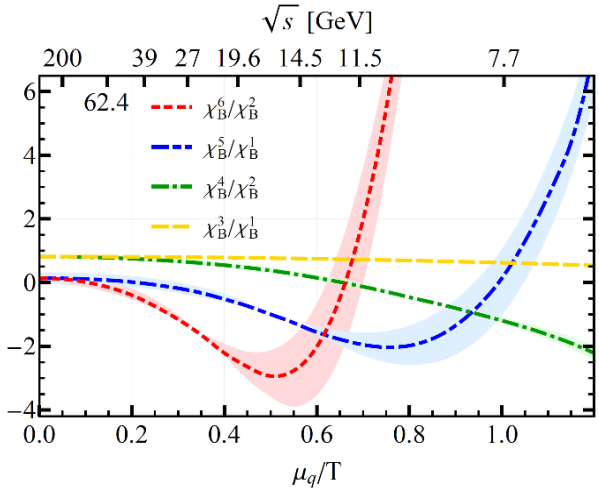

Figure 2: Higher order cumulant ratios in the PQM model along the freeze-out line.

References

[1] G. A. Almasi, B. Friman and K. Redlich, Phys. Rev. D 96, 014027 (2017)
[2] B. Friman, F. Karsch, K. Redlich and V. Skokov, Eur. Phys. J. C 71, 1694 (2011)

Experiment beamline: none
Experiment collaboration: none
Experiment proposal: none
Accelerator infrastructure: none
PSP codes: none
Grants: none
Strategic university co-operation with: Darmstadt

S-matrix approach to thermodynamics with structureless N-body scatterings

P. M. Lo[1,2]

[1]University of Wroclaw, PL-50204, Wroclaw, Poland; [2]GSI, Darmstadt, Germany

Structureless N-body scattering

According to the S-matrix formulation of statistical mechanics, the contribution to the thermodynamic pressure due to interactions takes the following form:

$$(\Delta \ln Z) = V \int \frac{d^3P}{(2\pi)^3} \frac{dM}{2\pi} e^{-\beta\sqrt{P^2+M^2}} B(M)$$
$$B(M) \equiv 2 \frac{\partial}{\partial M} Q(M).$$

Here B(M) is an effective spectral function and Q(M) is the corresponding phase shift function. For the case of elastic 2 -> 2 scattering processes, Q(M) can be formally identified with the usual scattering phase shift. In terms of quantum field theory amplitudes, we can write

$$Q(M) = \frac{1}{2} \mathrm{Im} \ln \left[1 + i \int d\phi_2 \, \mathcal{M} \right].$$

The amplitude can be constructed using the standard Feynman rules. The integration over the 2-body phase space means

$$\int d\phi_2 \, (\cdots) \to \int \frac{d^3p_1}{(2\pi)^3} \frac{1}{2E_1} \frac{d^3p_2}{(2\pi)^3} \frac{1}{2E_2} \times (2\pi)^4 \delta^4(P_I - \sum_i p_i) \, (\cdots).$$

The general N-body phase shift function Q(M) is difficult to obtain. However, if we restrict our attention to processes involving only structureless scatterings, that is, replacing the ampltidue with a (dimensionful) coupling constant

$$i\mathcal{M} = i \lambda_N,$$

the problem reduces to that of calculating the N-body phase space function. An efficient way to accomplish this task is to employ the Kallen expansion, which provides a recursive definition of the N-body phase space function via

$$\phi_N(s) = \frac{1}{16\pi^2 s} \int_{s'_-}^{s'_+} ds' \sqrt{\lambda(s, s', m_N^2)} \times \phi_{N-1}(s', m_1^2, m_2^2, ..., m_{N-1}^2),$$

To demonstrate how the N-body phase space function increases with s=M^2, we compute them numerically for a system of pions. The result is shown in Fig. [1].

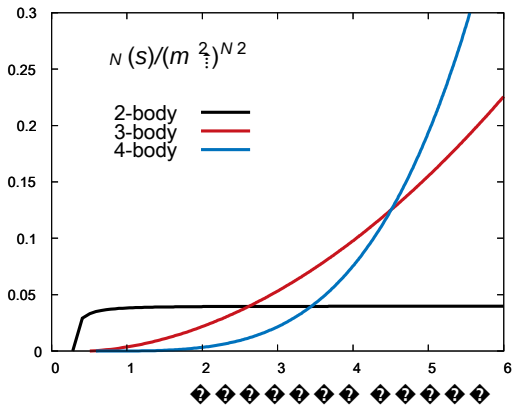

Figure 1: (N=2,3,4)-body phase space functions, scaled by the appropriate powers of pion mass, versus the center of mass energy sqrt(s).

From a purely kinematical point of view, effects from higher N-body phase space are generally suppressed compared to the lower ones at low invariant mass. However, their effects will show up and will eventually be dominating at high invariant masses in the manner dictated. In case of finite density or chemical potential, the takeover by higher N-body phase spaces can occur more rapidly due to the fugacity factor associated with an N-body state.

The phase space dominance model discussed here may be of interest to phenomenological studies. Performing modelling on the level of S-matrix elements or amplitudes, e.g. the invariant mass dependence of the coupling, can establish closer connection between observables and model parameters. Moreover, symmetries and physical conditions can be imposed on the S-matrix elements to constrain their functional form. Finally, we note that the purely kinematical consideration presented here can be non-trivially modified by interaction dynamics. [1]

References

[1] P. M. Lo, “S-matrix formulation of thermodynamics with N-body scatterings”, EPJC 77, 8, 533 (2017)

 DOI:10.15120/GR-2018-1

Experiment beamline: none
Experiment collaboration: none
Experiment proposal: none
Accelerator infrastructure: none
PSP codes: none
Grants: Maestro grant DEC-2013/10/A/ST2/00106
Strategic university co-operation with: none

Single electrons from open heavy-flavors in relativistic heavy-ion collisions

T. Song[1], H. Berrehrah[2], J. Torres-Rincon[2], L. Tolos[3], D. Cabrera[4], W. Cassing[1], and E. Bratkovskaya[2,5],

[1]Universität Gießen, Gießen, Germany; [2]Johann Wolfgang Goethe Universität, Frankfurt am Main, Germany;
[3]Campus Universitat Autonoma de Barcelona, Bellaterra, Spain;
[4]Centro Mixto Universidad de Valencia, Valencia, Spain; [5]GSI, Darmstadt, Germany.

We have studied the single electron spectra from D- and B-meson semileptonic decays in Au+Au collisions at $\sqrt{s_{NN}} = 200$, 62.4, and 19.2 GeV by employing the parton-hadron-string dynamics (PHSD) transport approach that has been shown to reasonably describe the charm dynamics at Relativistic-Heavy-Ion-Collider (RHIC) and Large-Hadron-Collider (LHC) energies on a microscopic level. In this approach the initial charm and bottom quarks are produced by using the PYTHIA event generator which is tuned to reproduce the fixed-order next-to-leading logarithm (FONLL) calculations for charm and bottom production. The produced charm and bottom quarks interact with off-shell (massive) partons in the quark-gluon plasma with scattering cross sections which are calculated in the dynamical quasi-particle model (DQPM) that is matched to reproduce the equation of state of the partonic system above the deconfinement temperature Tc. At energy densities close to the critical energy density ($\approx 0.5\ GeV/fm^3$) the charm and bottom quarks are hadronized into D- and B-mesons through either coalescence or fragmentation. After hadronization the D- and B-mesons interact with the light hadrons by employing the scattering cross sections from an effective Lagrangian. The final D- and B-mesons then produce single electrons through semileptonic decay.

Figures 1 and 2 show, respectively, the R_{AA} and v_2 of single electrons from D-meson and B-meson semileptonic decays in Au+Au collisions at $\sqrt{s_{NN}} = 200$ GeV. The shadowing effect enhances the bottom production and suppresses the charm production at low transverse momentum. The single electrons from B decay have a larger contribution than that from D decay above $p_T \approx 2.7 - 2.8\ GeV/c$. The dotted lines are the R_{AA} of single electrons including both shadowing and Cronin effects. Although the Cronin effect enhances the R_{AA}, it is not significant.

We have found that the PHSD approach well describes the nuclear modification factor R_{AA} and elliptic flow v_2 of single electrons in d+Au and Au+Au collisions at $\sqrt{s_{NN}}$ =200 GeV and the elliptic flow in Au+Au reactions at $\sqrt{s_{NN}} = 62.4$ GeV from the PHENIX collaboration, however, the large R_{AA} at $\sqrt{s_{NN}} = 62.4$ GeV is not described at all. Furthermore, we have made predictions for the R_{AA} of D-mesons and of single electrons at the lower energy of $\sqrt{s_{NN}} = 19.2$ GeV. Additionally, the medium modification of the azimuthal angle ϕ between a heavy quark and a heavy antiquark has been studied. We have found that the transverse flow enhances the azimuthal angular distributions close to $\phi = 0$ because the heavy flavors strongly interact with the medium in relativistic heavy-ion collisions and almost flow with the bulk matter.

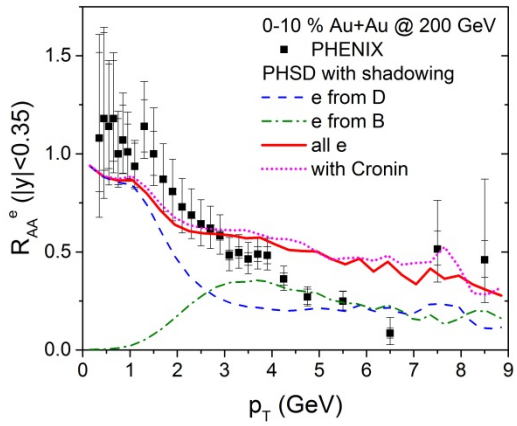

Figure 1: R_{AA} of single electrons from the semi-leptonic decay of D-mesons (dashed) and of B-mesons (dot-dashed) and the sum of them (solid) with shadowing effect in 0-10 % central Au+Au collisions at $\sqrt{s_{NN}} = 200$ GeV in comparison to the experimental data from the PHENIX collaboration. The dotted line is the R_{AA} including both shadowing and Cronin effects.

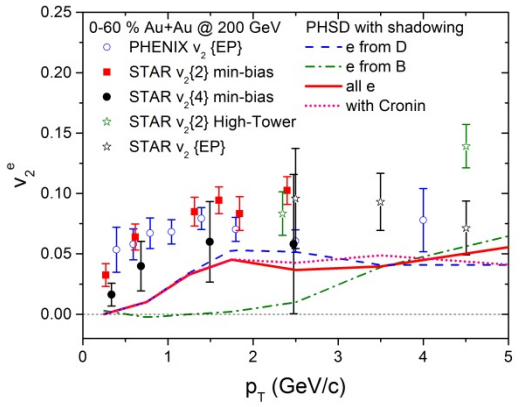

Figure 2: The elliptic flow v_2 of single electrons from the semi-leptonic decay of D-mesons (dashed) and of B-mesons (dot-dashed) and of both of them (solid) with shadowing effect in 0-60 % central Au+Au collisions at $\sqrt{s_{NN}} = 200$ GeV in comparison to the experimental data from the PHENIX and STAR collaborations. The dotted line is the v_2 of single electrons including both shadowing and Cronin effects.

References

[1] T. Song, H. Berrehrah, J. Torres-Rincon, L. Tolos, D. Cabrera, W. Cassing, E. Bratkovskaya, Phys. Rev. C96 (2017) 014905.

 DOI:10.15120/GR-2018-1

Foundations of the Trojan-Horse method

S. Typel[1,2]

[1]IKP, Technische Universität, Darmstadt, Germany; [2]GSI, Darmstadt, Germany

The Trojan-Horse (TH) method has been proposed by G. Baur in 1986 as an indirect approach to extract low-energy cross sections of a rearrangement reaction

$$A + x \rightarrow C + c \quad (1)$$

of astrophysical interest by studying the breakup reaction

$$A + a \rightarrow C + c + b \quad (2)$$

in the laboratory at much higher energies [1]. The TH nucleus a is assumed to be well described by a two-cluster system b+x where x is the transferred particle and b acts as a spectator. The connection of the cross section of reaction (1) with that of the surrogate reaction (2) was established with the help of direct reaction theory. This concept was already suggested in G. Baur's talk at the 1985 Varna International Summer School on Nuclear Physics [2]. The direct measurement of cross sections of reaction (1) at astrophysical energies is extremely difficult because of low-reaction rates and thus many experimental challenges arise. In contrast, reaction (2) is performed at energies above the Coulomb barrier without the strong suppression of the cross section caused by the Coulomb repulsion at very low energies. In addition, reaction (2) does not suffer from electron screening effects.

In the original proposal [1], G. Baur argued that the Fermi motion of x inside a would compensate the relative motion of A and x making small energies accessible in this system. However it was realized by Claudio Spitaleri and his group in Catania that the surrogate reaction (2) has to be studied at quasi-free scattering conditions, corresponding to a small momentum transfer to the spectator b, to exploit the virtues of the TH method, see, e.g., reference [3] and publications cited therein.

In first experimental attempts to apply the TH method it remained unclear how to establish the connection between the cross sections of reactions (1) and (2). Using detailed theoretical considerations [4,5] the cross section of reaction (2) could be factorized by employing a modified plane-wave impulse approximation (PWIA). The product contains a kinematic factor, the momentum distribution of relative motion $|\Phi_a(p_{bx})|^2$ of b and x inside a, and the half-off-shell cross section $d\sigma^{HOES}/d\Omega$ of reaction (1). The latter is related to the on-shell cross section by a simple penetrability factor. Applying this formulation, extensive applications of the TH method followed and low-energy cross sections of astrophysical reactions were determined with success, see, e.g., reference [6].

The conventional formulation of direct reaction theory for reaction (2) can be derived from the post form of the transition matrix element in distorted wave Born approximation (DWBA) with additional assumptions, in particular the so-called surface approximation. Formally, the matrix element is a first-order amplitude in reaction theory. The factors $|\Phi_a(p_{bx})|^2$ and $d\sigma^{HOES}/d\Omega$ can be related to two processes: the breakup of the Trojan horse a and reaction (1) as a subprocess of (2). Hence, the TH reaction can also be viewed as a two-step process with an intermediate off-shell propagation of the transferred particle x.

The connection between the one-step and two-step descriptions of the TH reaction was recently established in reference [7]. It was observed that the TH cross section is the direct part of the inclusive non-elastic breakup cross section. The corresponding transition matrix element contains the source function ρ with the exact three-body wave function. In the post representation within DWBA it has the Ichimura-Austern-Vincent form $\rho^{IAV}=\rho^{UT}+\rho^{HM}$ with two contributions. The Udagawa-Tamura term ρ^{UT} describes the elastic breakup of a and the fusion of x with A remaining in the ground state. The Hussein-McVoy term ρ^{HM} contains all other processes where A is excited or other channels in the A+x system are reached. The new formulation can be used for improvements in the analysis of experiments in order to access the validity of the approximations in the standard approach to the TH method.

References

[1] G. Baur. Phys. Lett. B 178 (1986) 135.
[2] G. Baur. Nuclear Energy 25 (1987) 183.
[3] S. Typel, EPJ Web Conf 165 (2017) 02008.
[4] S. Typel and H.H. Wolter, Few-Body Systems 29 (2000) 75.
[5] S. Typel and G. Baur, Annals Phys. 305 (2003) 228.
[6] C. Spitaleri et al., Eur. Phys. J. A 52 (2016) 77.
[7] C. A. Bertulani, M. S. Hussein, and S. Typel, Phys. Lett. B 776 (2018) 217.

Experiment beamline: none
Experiment collaboration: none
Experiment proposal: none
Accelerator infrastructure: none
PSP codes: none

Grants: DFG, SFB 1245
Strategic university co-operation with: none

Visualizing velocity field strengths with hyper-surfaces in spacetime

B. R. Schlei[1]

[1]GSI, Darmstadt, Germany

For questions: b.schlei@gsi.de

Abstract

One-dimensional (1D) time sequences of spatial, three-dimensional (3D) simulation or image data may implicitly carry dynamical information of their embedded subregions. Continuous hyper-surfaces can be constructed for the full 3+1D data that enclose certain spacetime regions. Here, we demonstrate that such hyper-surfaces may be viewed as 3D velocity vector fields, which explicitly characterize dynamically evolving 3D shapes contained in 4D.

Introduction

In this report, we consider the special case of 4D spacetime, where three dimensions refer to space, and a fourth dimension refers to time (i.e., 3+1D). E.g., relativistic hydrodynamical models that simulate relativistic heavy ion collisions may require the extraction of a so-called freeze-out hyper-surface (FOHS) from the 3+1D simulation data (*cf.*, e.g., Ref. [1] and Ref.s therein). The STEVE algorithm [2, 3] generates iso-valued hyper-surfaces that may implicitly be contained in four-dimensional (4D) data sets. A FOHS generated by STEVE consist of a finite set of tetrahedrons, which are embedded in 4D. For each tetrahedron (3-simplex), a covariant 4-normal, $d\sigma_\mu(x^\mu)=(d\sigma_x,d\sigma_y,d\sigma_z,d\sigma_t)$, at the contravariant event, $x^\mu=(x,y,z,t)$, with the three spatial cartesian coordinates x, y, and z, and the time t, respectively, can be calculated due to Ref. [2].

Approach and Results

Using the components of the 4-normals, let us define a 3-velocity

$$\vec{v}=(v_x,v_y,v_z)\equiv\frac{-d\sigma_t}{d\sigma_x^2+d\sigma_y^2+d\sigma_z^2}(d\sigma_x,d\sigma_y,d\sigma_z) \quad (1)$$

for each 3-simplex of a given hyper-surface that is embedded in 4D spacetime.

The magnitude $v=\sqrt{v_x^2+v_y^2+v_z^2}$ of each single 3-velocity, (*cf.*, Eq. (1)) can be encoded with a colour, which may then be assigned to its corresponding tetrahedron.

Fig.1 shows an example (*cf.*, also Ref. [2]) of a temporal sequence of intersections of a FOHS. The resulting 3D isothermes consist of triangles, which have inherited their colour from an intersected tetrahedron. In the figure, the colour red refers to regions of high speed, whereas the colour purple refers to zero and/or very low speeds.

We conclude our presentation with the notion that such processing may be useful also for medical applications [4], e.g., in the field of time-varying computed tomography [5].

References

[1] Yun Cheng, L. P. Csernai, V. K. Magas, B. R. Schlei, and D. Strottman, "Matching Stages of Heavy-Ion Collision Models," Phys. Rev. C81, 064910 (2010), doi: 10.1103/PhysRevC.81.064910.

[2] B. R. Schlei, "STEVE – Space-Time-Enclosing Volume Extraction", (2013) arXiv:1302.5683 [cs.CG].

[3] B. R. Schlei, "Method for Hypersurface Construction in N Dimensions", U.S. patent 9,607,431, Mar. 28, 2017; E.P. patent 2,715,673, Nov. 22, 2017.

[4] Private communication, C. Graeff, GSI.

[5] B. R. Schlei, "Flood fill segmentation for images from time-varying computed tomography", this GSI Scientific Report.

Experiment beamline: none
Experiment collaboration: none
Experiment proposal: none
Accelerator infrastructure: none
PSP codes: none
Strategic university co-operation with: none

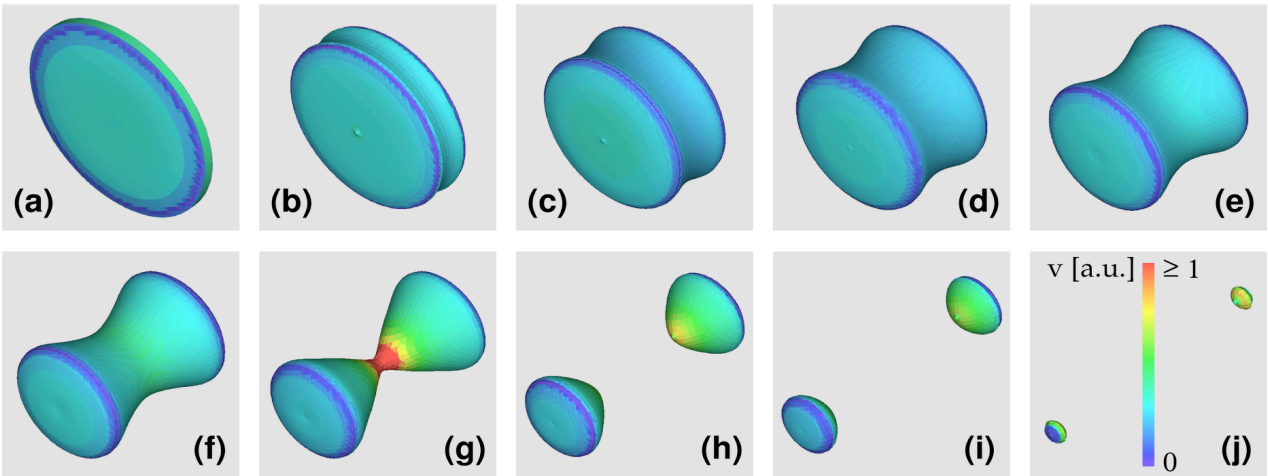

Figure 1: (a) – (j) Chronologically developing isothermes as a result of spatial hyper-surface intersections at equidistant times; (j) shows in addition a colour bar which decodes the relative velocity magnitudes of all images, (a) – (j). Note that the colour red refers to relative velocity magnitudes in the range of $[1.0,+\infty)$.

 DOI:10.15120/GR-2018-1

Parton-Hadron-Quantum-Molecular Dynamics (PHQMD) - a novel microscopic N-body transport approach for heavy-ion dynamics and hypernuclei production

E. Bratkovskaya[1,2], J. Aichelin[3] , A. LeFevre[1], V. Kireyev[4] , Y. Leifels[1]

[1]GSI, Darmstadt, Germany, [2]Johann Wolfgang Goethe Universität, Frankfurt am Main, Germany, [3]SUBATECH, Universite de Nantes, France, [4]Joint Institute for Nuclear Research, Russia

The formation of hypernuclei clusters in heavy-ion reactions has been a subject of many theoretical studies. Recent experimental results have shown that the hypernuclei and anti-hypernuclei can be produced in relativistic heavy-ion collisions (HIC) from SIS to LHC energies. Detailed investigations of the theoretical predictions have identified two sources of hypernuclei in these reactions:

a) In the overlap region of projectile and target, called participant region, strange baryons are produced in initial collisions between projectile and target nucleons. These strange baryons can migrate into the cold spectator matter where they can be absorbed and form heavy hypernuclei which have a rapidity close to projectile or target rapidity.

b) The Λ's may stay in the participant region, which expands and their interaction with the surrounding nucleons allows forming light clusters and hence lighting hypernuclei. In view of their small binding energy and their hot environment, this is like the creation of “ice in a fire”. Nevertheless, such hypernuclei have been found around mid-rapidity in RHIC and LHC experiments, a phenomenon which awaits an explanation.

In addition, the production of both types of hypernuclei may shed light on our theoretical understanding of the dynamics of heavy-ion reactions, which cannot be addressed by other probes. In particular, the formation of heavy projectile/target like hypernuclei elucidates the physics at the interface between spectator and projectile matter. Since the strange baryon comes necessarily from the overlap region the multiplicity as well as the rapidity distribution of the hypernuclei is related to the probability that strange baryons of a given rapidity are absorbed by the spectator matter by means of their potential interaction with the cold spectator matter. On the other hand, mid-rapidity hypernuclei test the phase space distribution of baryons in the expanding participant matter, especially whether strange and non strange baryons are in thermal equilibrium and whether their space time distribution is similar. This may contribute to clarifying the origin of their formation.

We have developed the novel microscopic n-body dynamical transport approach PHQMD (Parton-Hadron-Quantum-Molecular-Dynamics) for the description of particle production and cluster formation in heavy-ion reactions at relativistic energies. The PHQMD extends the established PHSD (Parton-Hadron-String-Dynamics) transport approach by introducing n-body quantum molecular dynamic type propagation of hadrons. This allows for a dynamical description of cluster formation based on the FRIGA (‘Fragment Recognition In General Application’) model. It keeps the collision integral (which describes the particle collisions) of the PHSD. This allows to use the PHQMD transport approach in different modes: the mean-field based PHSD mode and the QMD mode based on two and three-body potential interactions between the nucleons and, thus, to study the sensitivity of observables for the different ways of the description of the heavy-ion dynamics.

The PHQMD includes the following features for the dynamical fragment identification: the final fragment yield can either be determined with a minimum spanning tree (MST) procedure [2] or with cluster finding algorithms based on the Simulated Annealing Clusterization Algorithm (FRIGA) [3]. First results from combining the PHSD with the FRIGA code have been reported in [4].

In Figure 1 we validate our approach by showing that we can reproduce the complex fragment pattern observed by the ALADIN collaboration at the highest energies where experimental data for heavy fragments are available. These heavy fragments have a rapidity close to beam and target rapidity and with increasing energy also hyperfragments can be formed in this kinematical region.

Within the PHQMD we have obtained the first results for hadronic 'bulk' observables - as clusters production at SIS and FAIR/NICA energies, rapidity distributions and transverse mass spectra [5].

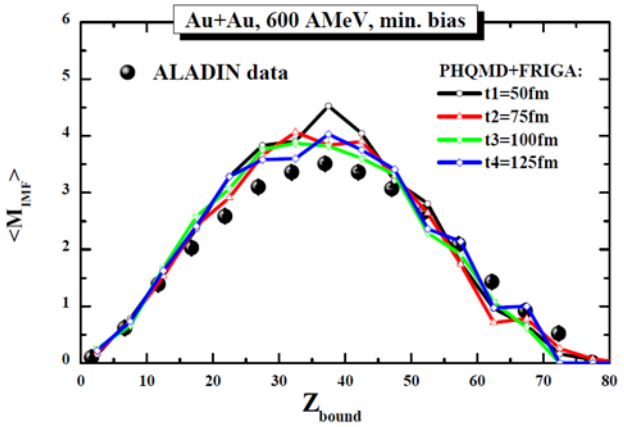

Figure 1: Rise and fall of the multiplicity of intermediate mass fragments as a function of the total bound charge. Both quantities are measured for forward emitted fragments. We compare the results of PHQMD for different times to identify fragments with the experimental data [1].

References

[1] A. Schuttauf et al., Nucl. Phys. A 607 (1996) 457.
[2] J. Aichelin, Phys. Rept. 202 (1991) 233.
[3] R. K. Puri, J. Aichelin, J. Comput. Phys. 162, 245 (2000).
[4] A. Le Fevre et al., J. Phys. Conf. Ser. 668, 012021 (2016).
[5] E.Bratkovskaya eta al., in preparation.

Production of light r-process elements in blue kilonova

S. Nikas[1,2], G. Martinez-Pinedo[1,2], A. Sieverding[1,2]

[1]GSI, Darmstadt, Germany; [2]TU Darmstadt, Darmstadt, Germany;

The r-process is responsible for the production of about half of the heavy elements observed in the solar abundances. The site of the r-process was unknown until recent observations. The gravitational wave event GW170817, which was identified as a binary Neutron Star Merger (NSM), was followed by the detection of an electromagnetic counterpart (EM170817) that is consistent with predictions for a kilonova/macronova associated with r-process nucleosynthesis [1,2]. In particular the observation of a bright fast fading UV component.

Since the complicated atomic structure of lanthanides implies high opacity ejecta, this indicates the presence of material with relatively high electron fractions and consequently low lanthanide production[3,4,5]. While the distinction between s and r-process produced elements is well defined for heavy elements, this is not the case for lighter elements. This is also partly due to the impact of other proposed processes like the i-process and the νp-process that are thought to have a contribution in this region. We study the nucleosynthesis for the conditions of high Ye outflows from NSMs to try to see if this could be the site for the production of the r-process abundance pattern for A <100.

Calculations-Results

We use a range of Ye (0.35, 0.36, 0.37, 0.38) which we average with ejecta velocity v/c = 0.2 and entropy 15 k_B per baryon following the presciption of [7]. Figure 1 shows that we can reproduce the peaks seen A=80 and A=84 in the r-process abundance pattern and have an overall agreement in the region. The details of the r-process abundance pattern are very sensitive to the nuclear physics underlying this process. Nuclear information (namely: masses, beta decay rates, and neutron capture rates) in this region are not known for all the neutron rich nuclei participating in the r-process. As a result of ongoing experimental campaigns more and more data becomes available. With the current knowledge of nuclear physics underlying this process we can conclude that we can not exclude NSM as the source of light r-process elements but a final conclusion require a better understanding of the properties of n-rich nuclei.

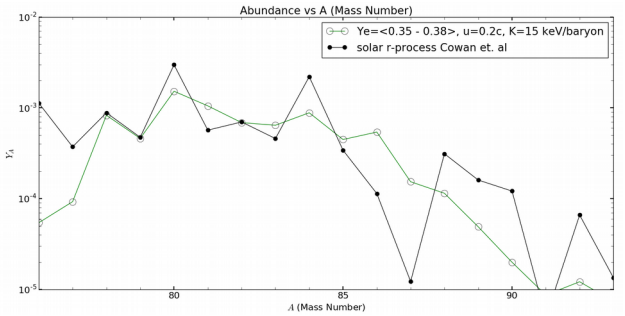

Figure 1: Filled black circles represent the r-process abundances as presented in the paper of Cowan et al. [6] Green open circles represent the average abundance for Ye between 0.35 and 0.38, ejecta velocity of 0.2c and entropy of 15 keV per baryon.

References

[1] Metzger, B. D., et al. "Electromagnetic counterparts of compact object mergers powered by the radioactive decay of r-process nuclei." Monthly Notices of the Royal Astronomical Society 406.4 (2010): 2650-2662.

[2] Kasliwal, M. M., et al. "Illuminating gravitational waves: a concordant picture of photons from a neutron star merger."Science 358.6370 (2017): 1559-1565.

[3] Evans, P. A., et al. "Swift and NuSTAR observations of GW170817: Detection of a blue kilonova."Science 358.6370 (2017): 1565-1570.

[4] Metzger, Brian D., and Edo Berger. "What is the most promising electromagnetic counterpart of a neutron star binary merger?." The Astrophysical Journal 746.1 (2012): 48.

[5] Joel de Jesús Mendoza-Temis, Joel, et al. "Nuclear robustness of the r process in neutron-star mergers." Physical Review C 92.5 (2015): 055805.

[6] Cowan, John J., et al. "R-process abundances and chronometers in metal-poor stars." The Astrophysical Journal 521.1 (1999): 194.

[7] S Rosswog et al 2017 "Detectability of compact binary merger macronovae" Class. Quantum Grav. 34 104001

Experiment beamline: none
Experiment collaboration:other: / none
Experiment proposal: none
Accelerator infrastructure:other: / none
PSP codes: none
Grants:
Strategic university co-operation with: Darmstadt

 DOI:10.15120/GR-2018-1

Short-range and tensor correlations in back-to-back nucleon pairs

T. Neff[1], and H. Feldmeier[1,2]

[1]GSI, Darmstadt, Germany; [2]FIAS, Frankfurt, Germany

Short-range correlations (SRC) in nuclei reflect the repulsive core and the strong tensor component of the nucleon-nucleon interaction. To study SRC in nuclei we combine many-body calculations in the ab-initio no-core shell model with unitarily transformed interactions and operators using the similarity renormalization group (SRG). The SRG transformation softens the interaction and makes solving the many-body problem possible. It is important to note that a consistent approach requires that not only the Hamiltonian but also all operators are transformed. Due to the short-range nature of the transformation long-range observables like radii or electromagnetic transition strengths are only weakly sensitive to the transformation. The situation is totally different for observables that are sensitive to the short-range behaviour of the wave function.

This is the case for the high-momentum components that are also studied in great detail experimentally. Up to now one of the clearest approaches have been (e,e'NN) reactions, i.e. the knockout of nucleon pairs by electrons. The experimental information has to be compared to theoretical predictions and it is important to identify as clearly as possible the experimental and theoretical observables. In the knockout process nucleon-nucleon pairs are observed as a function of relative momentum. However there are experimental cuts that restrict the total pair momenta. That the relative momentum distributions depend very strongly on the pair momentum is shown in Fig. 1 where we show the contributions to the total relative momentum distributions from nucleon pairs with total spin S and total isospin T in the alpha particle as a function of relative momentum. The first observation is that the momentum distributions are very different from what would be expected in a mean-field description. In this simple picture the contributions of the two even channels (S,T)=(1,0) and (S,T)=(0,1) would be both 0.5 independent from relative momentum. The contributions from the odd channels would be zero. What we observe is quite different. The situation is very clear for back-to-back pairs shown on the bottom. Here we find a situation close to what would be expected in the mean-field for pairs with relative momentum well below Fermi momentum. Around Fermi momentum however almost all pairs found are deuteron-like (S,T)=(1,0). This is caused by tensor correlations that dominate in that momentum region. We observe similar but not identical results for the different interactions. The situation is much more complicated when we do not restrict the total momentum as shown on top. Whereas back-to-back pairs only show two-body correlations we find significant contributions from many-body correlations if we look at all pairs. These are especially visible in the significant contribution of (S,T)=(1,1) pairs that can be traced backed to three-body correlations induced by the tensor force. In Fig. 2 we show the same information in a different way that allows to compare with experimental data from JLAB measuring the ratio of proton-proton to proton-neutron pairs as a function of relative momentum.

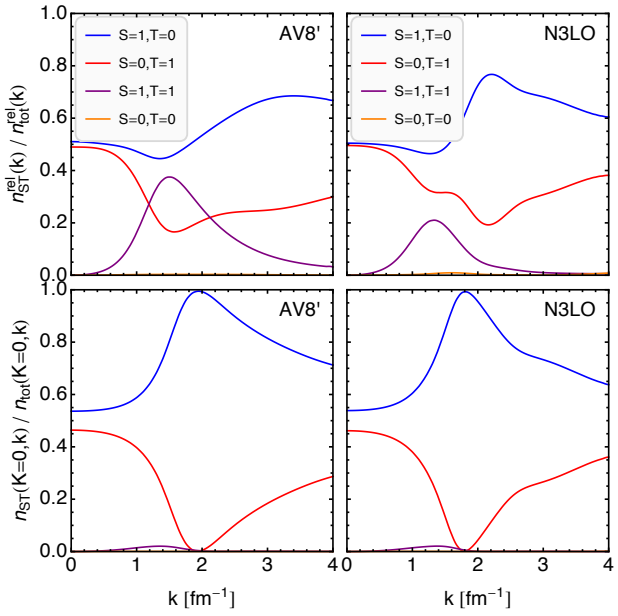

Figure 1: Contribution of the different spin-isospin channels to the total relative momentum distribution as a function of relative momentum. On top for all pair momenta, on the bottom for back-to-back pairs only. On the left for the AV8' interaction on the right for the N3LO interaction.

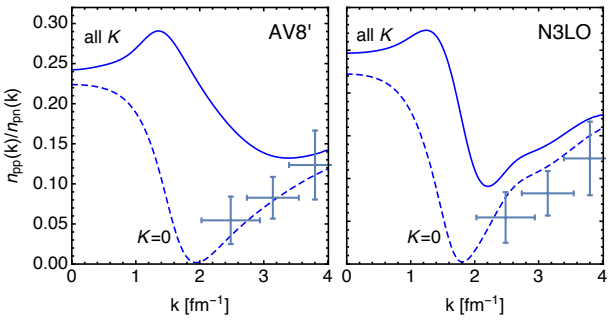

Figure 2: Ratio of proton-proton pairs to proton-neutron pairs for the AV8' interaction on the left and the N3LO interaction on the right. Full curves show the ratio for all pairs, dashed curves show the ratio for the back-to-back pairs. Experimental data are from [2]

References

[1] T. Neff, H. Feldmeier, W. Horiuchi, Phys. Rev. C 92, 024003 (2015)

[2] I. Korover et al. (Jefferson Lab Hall A Collaboration), Phys. Rev. Lett. 113, 022501 (2014).

Implementation of conservation laws at transition from hydrodynamics to microscopic transport in heavy ion collisions

C. Schwarz [1,2], D. Oliinychenko [1], L.-G. Pang[1], S. Ryu[1] and H. Petersen[1,2,3]

[1]Frankfurt Institute for Advanced Studies, Ruth-Moufang-Straße 1, 60438 Frankfurt am Main, Germany
[2]Institut für Theoretische Physik, Goethe-Universität, Max-von-Laue-Straße 1, 60438 Frankfurt am Main, Germany
[3]GSI Helmholtzzentrum für Schwerionenforschung GmbH, Planckstraße 1, 64291 Darmstadt, Germany

Heavy ion collisions, at the Relativistic Heavy Ion Collider (RHIC) and the Large Hadron Collider (LHC), are experimental tools to explore high-temperature QCD matter. Realistic dynamical models are indispensable to connect the experimental results with the properties (equation of state and transport coefficients) of hot QCD matter.

The current state-of-the-art are so called hybrid approaches, which combine viscous hydrodynamics and microscopic transport to take increasing mean free path into account. The transition from hydrodynamics to microscopic transport (dubbed 'particlization') is based on the Cooper-Frye formalism [1], which provides a connection between Boltzmann distribution function and momentum-space distribution emerging from specific 3-dimensional hypersurface such that energy and momentum are conserved.

$$\frac{dN}{d^3p} = \frac{d}{(2\pi)^3}\int_\Sigma f(x,p)\frac{p^\mu d^3\Sigma_\mu}{E_p} \quad (1)$$

where d and Σ are respectively degeneracy and hypersurface.

The simplest way to implement this formalism, which is also used in Ref. [2], is to sample each species at each space-time point independently, assuming grand canonical ensemble. Conservation of charges, energy and momentum is achieved only on average over events. This so-called “conventional” sampling starts by multiplicity sampling from Poisson distribution with average

$$\langle N_i\rangle_{1-cell} = d_i\left[\int \frac{d^3k}{(2\pi)^3} f_i(k)\right] u^\mu \Delta\Sigma_\mu \quad (2)$$

where u^μ and $\Delta\Sigma_\mu$ are the flow velocity and normal vector of the hypersurface, respectively. Then, the momenta of particles are sampled from the distribution function $f(x,p)$ near thermal equilibrium.

Even though the conventional way of particlization, in conjunction with oversampling, can be used to study single-particle distribution, the event-by-event conservation must be ensured to investigate fluctuations and correlations. It is shown in [3] that charge and energy can be globally conserved in each event by the Single Particle Rejection with Exponential Weights (SPREW) method.

To implement global charge conservation in the SPREW sampling, the average of conserved charge X (baryon number B, strangeness S and electric charge Q) is evaluated according to

$$X_{surface} = \sum_i X_i d_i \int_\Sigma n_i(x)\, u^\mu d^3\Sigma_\mu \quad (3)$$

where the summation goes over all particles species. If the newly sampled particle would result in larger deviations of the total charge from its average value (i.e., $X_{new\ particle}$ and $X_{sample} - X_{surface}$ have the same sign), it is rejected with the following probability.

$$P_{reject} = 1 - e^{-|X_{sample} - X_{surface}|} \quad (4)$$

After momenta are sampled in the same way as the conventional sampling, they are rescaled for energy conservation.

$$E_{surface} = \sum_n \sqrt{(1+a)^2 p_n^2 + m_n^2} \quad (5)$$

In the case of Au-Au collisions, the typical value of a is very small ($|a| \simeq 3$ %). Therefore, one finds that charge conservation does not lead to significant deformation of momentum-space distribution. Figure 1 shows global baryon number conservation in the SPREW sampling algorithm. These conservation laws are important for the fluctuation observables to measure the phase transition as it will be done at FAIR.

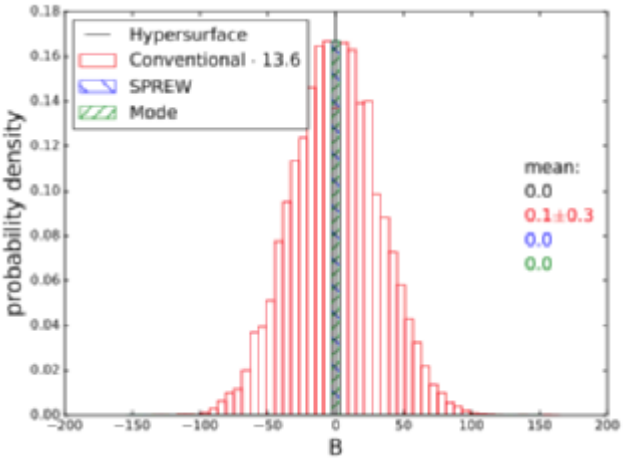

Figure 1: Probability distribution of net baryon number in Au-Au collisions with $\sqrt{s_{NN}} = 200$ GeV. Taken from Ref. [3].

References

[1] F. Cooper and G. Frye, Phys. Rev. D 10, 186 (1974).
[2] S. Ryu, J.-F. Paquet, C. Shen, G. S. Denicol, B. Schenke, S. Jeon and C. Gale, Phys. Rev. Lett. 115, no. 13, 132301 (2015) [arXiv:1502.01675 [nucl-th]].
[3] C. Schwarz, D. Oliinychenko, L.-G. Pang, S. Ryu and H. Petersen, J. Phys. G 45, no. 1, 015001 (2018) [arXiv:1707.07026 [hep-ph]].

Grants: Helmholtz Young Investigator Group VH-NG-822 from the Helmholtz Association and GSI

 DOI:10.15120/GR-2018-1